Available online at www.sciencedirect.com
SCIENCE DIRECT®
International Journal of Solids and Structures 42 (2005) 4220–4238
INTERNATIONAL JOURNAL OF SOLIDS and STRUCTURES
www.elsevier.com/locate/ijsolstr

Exact solutions for the buckling of rectangular plates having linearly varying in-plane loading on two opposite simply supported edges

Jae-Hoon Kang [a,*], Arthur W. Leissa [b]

[a] Department of Architectural Engineering, School of Architecture and Building Science, College of Engineering, Chung-Ang University, 221 Heuksuk-Dong, Dongjak-Ku, Seoul 156-756, South Korea
[b] Department of Mechanical Engineering, Colorado State University, Fort Collins, Colorado, CO 80523-1374, USA

Received 21 April 2004; received in revised form 11 August 2004
Available online 21 January 2005

Abstract

An exact solution procedure is formulated for the buckling analysis of rectangular plates having two opposite edges ($x = 0$ and a) simply supported when these edges are subjected to linearly varying normal stresses $\sigma_x = -N_0[1-\alpha(y/b)]/h$, where h is the plate thickness. The other two edges ($y = 0$ and b) may be clamped, simply supported or free, or they may be elastically supported. By assuming the transverse displacement (w) to vary as, $\sin(m\pi x/a)$, the governing partial differential equation of motion is reduced to an ordinary differential equation in y with variable coefficients, for which an exact solution is obtained as a power series (i.e., the method of Frobenius). Applying the boundary conditions at $y = 0$ and b yields the eigenvalue problem of finding the roots of a fourth order characteristic determinant. Care must be exercised to retain sufficient terms in the power series in calculating accurate buckling loads, as is demonstrated by a convergence table for all nine possible combinations of unloaded clamped, simply supported or free edges at $y = 0$ and b. Buckling loads are presented for all nine possible edge combinations over the range of aspect ratios $0.5 \leqslant a/b \leqslant 3$ for loading parameters $\alpha = 0$, 0.5, 1, 1.5, 2, for which $\alpha = 2$ is a pure in-plane bending moment. Some interesting contour plots of their mode shapes are presented for a variety of edge conditions and in-plane moment loadings. Because the nondimensional buckling parameters depend upon the Poisson's ratio (ν) for five of the nine edge combinations, results are shown for them for the complete range, $0 \leqslant \nu \leqslant 0.5$ valid for isotropic materials. Comparisons are made with results available in the published literature.

Keywords: Buckling; Rectangular plate; Exact solution; Frobenius method; In-plane buckling load; Linearly varying in-plane load

* Corresponding author. Tel.: +82 2 820 5342; fax: +82 2 812 4150.
E-mail address: jhkang@cau.ac.kr (J.-H. Kang).

0020-7683/$ - see front matter © 2004 Elsevier Ltd. All rights reserved.
doi:10.1016/j.ijsolstr.2004.12.011

Nomenclature

a, b	plate lengths in x- and y-directions, respectively (cf. Fig. 1)
$C_{m,n}$	arbitrary coefficient in Eq. (10)
C, F, S	clamped, free, and simply supported edge indicator, respectively
D	flexural rigidity of plate $[\equiv Eh^3/12(1-\nu^2)]$
E	Young's modulus
h	plate thickness
k	plate aspect ratio $(\equiv a/b)$
m	numbers of half-waves in the x-direction of a buckling mode shape
M	in-plane moment applied to each of the simply supported ends
M^*	nondimensional in-plane moment $(\equiv M/D = N_0^*/6)$
M_{cr}	critical buckling in-plane moment
M_{cr}^*	nondimensional critical buckling in-plane moment $(\equiv M_{cr}/D)$
M_y	bending moment per unit distance on y-plane
n	non-negative integer in Eq. (10)
N	upper limit of the summation in Eq. (10)
N_0	intensity of compressive force at $y = 0$
N_{0cr}	critical buckling intensity of compressive force at $y = 0$
N_0^*	nondimensional intensity of compressive force at $y = 0$ $(\equiv N_0 b^2/D)$
N_{0cr}^*	nondimensional critical buckling intensity of compressive force at $y = 0$ $(\equiv N_{0cr\ b}{}^2/D)$
N_x, N_y	normal forces per unit distance on x- and y-planes, respectively
N_{xy}	shear force per unit distance on x-plane and parallel to y-axis
V_y	effective shear force per unit distance on y-plane
w	transverse plate deflection
x, y	rectangular coordinates with origin at plate corner (cf. Fig. 1)
Y_m	deflection function of η,
Y_m'', Y_m^{IV}	the second and fourth derivatives of Y_m with respect to η, respectively
α	numerical loading factor in Eq. (3) (cf. Fig. 2)
β_m	$\equiv m\pi/k (m = 1, 2, 3\ldots)$
ν	Poisson's ratio
ξ, η	nondimensional coordinates for x and y, defined by x/a and y/b, respectively
π	3.141592...
σ_x, σ_y, σ_{xy}	in-plane stress components
∇^4	bi-harmonic operator $(\equiv \partial^4/\partial x^4 + 2\partial^4/\partial x^2\partial y^2 + \partial^4/\partial y^4$ in rectangular coordinates)

1. Introduction

For more than a century researchers in structural mechanics throughout the world have endeavored to obtain accurate theoretical results for the critical buckling loads of plates, as well as their corresponding buckling mode shapes. Several thousands of research papers on these topics have appeared in the international scientific and technical journals and in conference proceedings, most of them dealing with rectangular plates. Much of the useful results has been summarized in many texts and handbooks (Timoshenko and Gere, 1963; Volmir, 1967; Bulson, 1970; Japan Column Research Council, 1971; Szilard, 1974; Brush and Almroth, 1975; Trahair and Bradford, 1998).

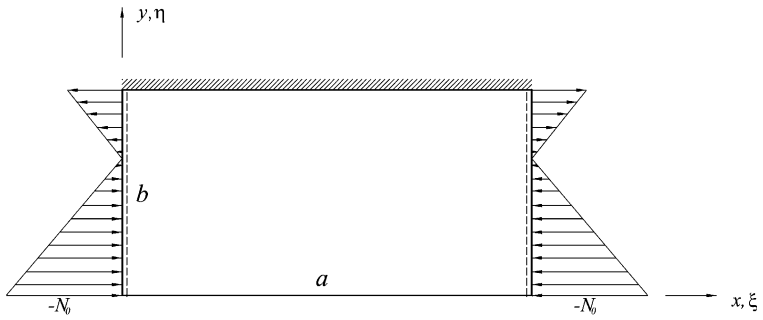

Fig. 1. An S-F-S-C plate with linearly varying in-plane loads, with coordinate convention.

Rectangular plates subjected to uniform in-plane stresses have been extensively analyzed in the buckling literature because the governing differential equation of equilibrium has constant coefficients, yielding exact solutions for buckling loads straightforwardly when two opposite edges of the plates are simply supported.

Of course, a plate may be loaded at two opposite edges by non-uniform, in-plane, axial forces (N_x), the first variation from the uniform loading being one which varies linearly. A special case of this is a pure, in-plane bending moment. In the non-uniform loading case the analysis is more formidable, and exact solutions are much more difficult to achieve. One finds considerable approximate results for plate buckling loads for such non-uniform stress fields, typically obtained by energy methods. Recently, for the case of linearly varying in-plane loadings some researchers have presented approximate results (Smith et al., 1999a,b; Bradford et al., 2000; Smith et al., 2000). Exact solutions for S-F-S-F (Kang and Leissa, 2001) and S-C-S-C plates (Leissa and Kang, 2002) have also been obtained, where two opposite edges are simply supported and the other two are either free (F) or clamped (C).

Some researchers have also analyzed both the buckling and vibration of rectangular plates subjected to in-plane stress field (Kang and Leissa, 2001; Leissa and Kang, 2002; Bassily and Dickinson, 1972, 1978; Dickinson, 1978; Kielb and Han, 1980; Kaldas and Dickinson, 1981). Bifurcation buckling may be regarded as a special case of the vibration problem; that is, determining the in-plane stresses which cause vibration frequencies to reduce to zero.

The present work presents exact solutions for the buckling loads and mode shapes for rectangular plates having two opposite edges simply supported when these edges are subjected to linearly varying in-plane

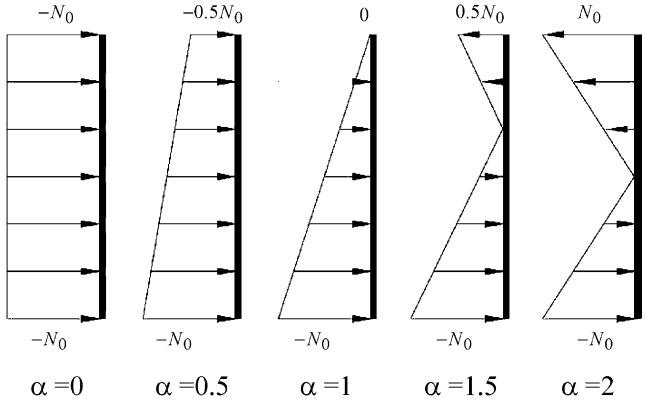

Fig. 2. Examples of in-plane loading N_x along the edge $x = 0$.

Table 1
Convergence of nondimensional critical buckling moments M^*_{cr} of rectangular plates with two opposite edges simply-supported for $a/b = 2.3$, $\alpha = 2$, and $\nu = 0.3$ by the power series method

N[a]	S-C-S-C ($m = 5$)	S-C-S-S ($m = 5$)	S-C-S-F ($m = 5$)	S-S-S-C ($m = 4$)	S-S-S-S ($m = 3$)	S-S-S-F ($m = 3$)	S-F-S-C ($m = 1$)	S-F-S-S ($m = 1$)	S-F-S-F ($m = 1$)
5	–[b]	–	–	–	–	–	1.615	0.5771	0.2498
7	16.02	–	–	–	6.543	–	3.017	1.312	0.6253
9	3.764	–	–	38.27	7.025	26.95	3.352	1.660	1.067
11	1.204	–	–	–	53.58	–	3.779	1.903	1.424
13	0.07537	–	–	51.81	34.94	36.03	3.908	1.983	1.583
15	0.9309	0.4502	–	–	3356	120.6	3.923	1.993	1.606
17	2.263	1.498	0.6914	87.92	15.36	43.03	3.925	**1.994**	**1.610**
19	4.112	2.984	1.821	670.5	20.78	40.60	**3.925**	1.994	1.610
21	6.619	5.050	3.562	145.4	139.8	36.88	3.925	1.994	1.610
23	9.909	7.832	6.161	–	536.2	37.47	3.925	1.994	1.610
25	14.08	11.45	10.01	157.6	42.50	37.69	3.925	1.994	1.610
27	19.23	16.02	16.13	130.8	38.17	39.05	3.925	1.994	1.610
29	25.40	21.62	571.5	42.37	39.45	39.48	3.925	1.994	1.610
31	32.58	28.33	576.2	40.55	39.87	39.68	3.925	1.994	1.610
33	40.62	36.11	511.2	40.17	39.84	39.73	3.925	1.994	1.610
35	49.06	44.74	600.7	40.08	**39.83**	39.74	3.925	1.994	1.610
37	56.75	53.41	514.5	40.07	39.83	**39.75**	3.925	1.994	1.610
39	62.01	60.26	505.9	**40.06**	39.83	39.75	3.925	1.994	1.610
41	64.29	63.73	486.4	40.06	39.83	39.75	3.925	1.994	1.610
43	64.94	64.80	473.5	40.06	39.83	39.75	3.925	1.994	1.610
45	65.09	65.06	66.00	40.06	39.83	39.75	3.925	1.994	1.610
47	**65.12**[c]	65.11	65.27	40.06	39.83	39.75	3.925	1.994	1.610
49	65.12	**65.12**	65.14	40.06	39.83	39.75	3.925	1.994	1.610
51	65.12	65.12	65.12	40.06	39.83	39.75	3.925	1.994	1.610
53	65.12	65.12	**65.11**	40.06	39.83	39.75	3.925	1.994	1.610
55	65.12	65.12	65.11	40.06	39.83	39.75	3.925	1.994	1.610

[a] N = total number of polynomial terms used in the power series method.
[b] The symbol (–) means that no roots were found.
[c] The nondimensional critical buckling moments in bold and underlined indicate the best convergent values in each column with the smallest N.

normal stresses. The procedure is applied to all possible combinations of clamped, simply supported or free edge conditions applied continuously along the other unloaded edges. For the case of opposite edges being simply supported, a variables separable solution exists, which reduces the partial differential equation to an ordinary one having variable coefficients. This is solved by the classical power series method of Frobenius, and the convergence of the series is established. Comparisons are also made with results available in the published literature.

2. Analysis

Consider a rectangular plate of lateral dimensions $a \times b$, as shown in Fig. 1, having its edges $x = 0$ and $x = a$ simply supported and linearly varying in-plane stresses acting along these two edges, whereas the other two edges ($y = 0$ and $y = b$) may be either clamped (C), simply supported (S), or free (F), and have no in-plane stresses. Assuming that the plate is thin, has uniform thickness, and that its material is homogeneous, isotropic and linearly elastic, the differential equation of motion governing buckling is

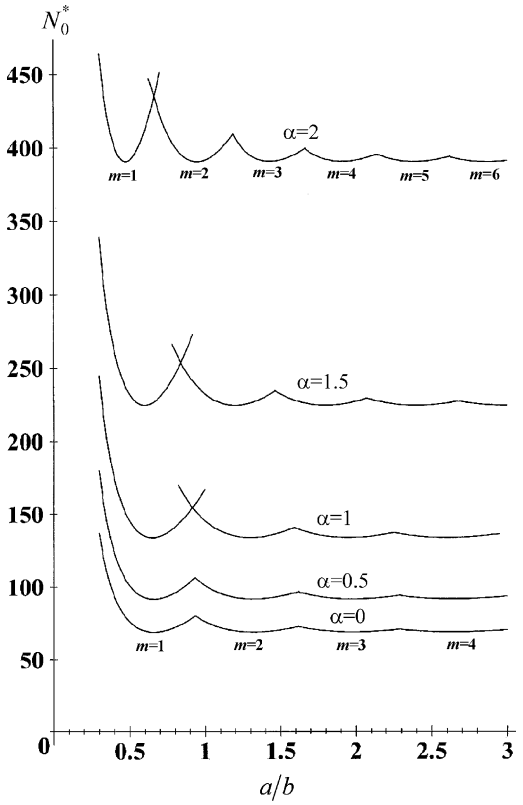

Fig. 3. Nondimensional buckling in-plane loads $N_0^* \equiv N_0 b^2/D$ vs. aspect ratio $k \equiv a/b$ for S-C-S-C plates (all v).

$$D\nabla^4 w = N_x \frac{\partial^2 w}{\partial x^2} + 2N_{xy} \frac{\partial^2 w}{\partial x \partial y} + N_y \frac{\partial^2 w}{\partial y^2}, \tag{1}$$

where w is transverse displacement; ∇^4 is the biharmonic differential operator (i.e., $\partial^4/\partial x^4 + 2\partial^4/\partial x^2 \partial y^2 + \partial^4/\partial y^4$ in rectangular co-ordinates); D is the flexural rigidity of the plate defined by

$$D \equiv \frac{Eh^3}{12(1-v^2)}, \tag{2}$$

E is Young's modulus; h is the plate thickness; v is Poisson's ratio; N_x and N_y are normal forces per unit length of plate in the x and y directions, respectively, positive if in *tension*; and N_{xy} is shearing force per unit length in the xy-plane. The forces (per unit length) are related to the in-plane stresses $(\sigma_x, \sigma_y, \tau_{xy})$ by $N_x = \sigma_x h, N_y = \sigma_y h$, and $N_{xy} = \tau_{xy} h$.

Let us assume $N_y = N_{xy} = 0$ and express N_x by the linear variation

$$N_x = -N_0\left(1 - \alpha\frac{y}{b}\right), \tag{3}$$

where N_0 is the intensity of compressive force at $y = 0$, and α is a numerical loading factor. This stress distribution is applied at the ends of the plate ($x = 0, x = a$), remains the same within its interior, and satisfies the plane elasticity equations exactly. By changing α, we can obtain various particular cases. For example, by taking $\alpha = 0$ we have the case of uniformly distributed compressive force. When $\alpha = 1$, the compressive

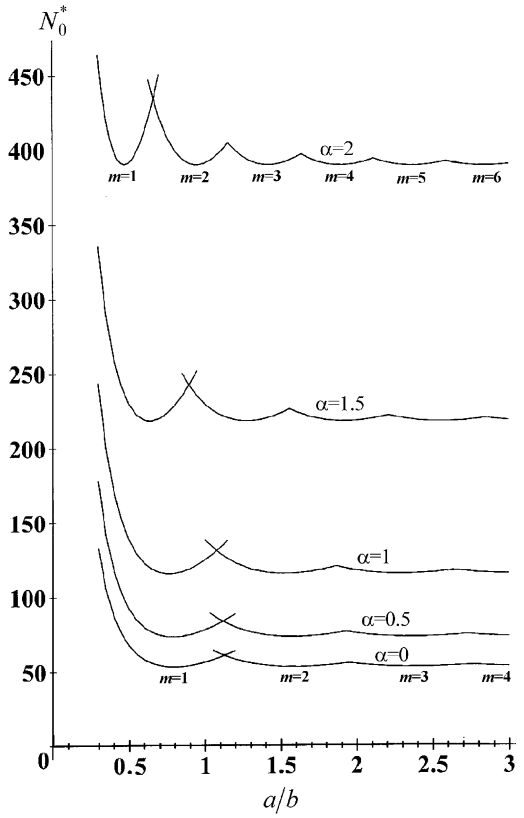

Fig. 4. Nondimensional buckling in-plane loads $N_0^* \equiv N_0 b^2/D$ vs. aspect ratio $k \equiv a/b$ for S-C-S-S plates (all ν).

force varies linearly from $-N_0$ at $y = 0$ to zero at $y = b$. For $\alpha = 2$ we obtain the case of pure in-plane bending. With other α in the range $0 < \alpha < 2$, we have a combination of bending and compression. Examples of these cases are shown in Fig. 2. For $\alpha < 0$ or $\alpha > 2$ the problems arising are identical with ones having $0 < \alpha < 2$ if the edge conditions at $y = 0$ and b are considered properly. The governing equation of motion (1) then reduces to

$$\nabla^4 w + \frac{N_0}{D}\left(1 - \alpha\frac{y}{b}\right)\frac{\partial^2 w}{\partial x^2} = 0. \tag{4}$$

Adopting the nondimensional coordinates $\xi \equiv x/a$ and $\eta \equiv y/b$, Eq. (4) becomes

$$\frac{\partial^4 w}{\partial \xi^4} + 2k^2\frac{\partial^4 w}{\partial \xi^2 \partial \eta^2} + k^4\frac{\partial^4 w}{\partial \eta^4} + \frac{a^2 N_0}{D}(1 - \alpha\eta)\frac{\partial^4 w}{\partial \xi^4} = 0, \tag{5}$$

where $k = a/b$ is the plate aspect ratio.

A solution for the displacement w may be taken as:

$$w(\xi, \eta) = Y_m(\eta)\sin(m\pi\xi), \tag{6}$$

where Y_m is a function of η, and m the numbers of half-waves in mode shapes in the x direction. Eq. (6) satisfies exactly the simply-supported boundary conditions at $\xi = 0$ and 1. Substituting Eq. (6) into (5) yields

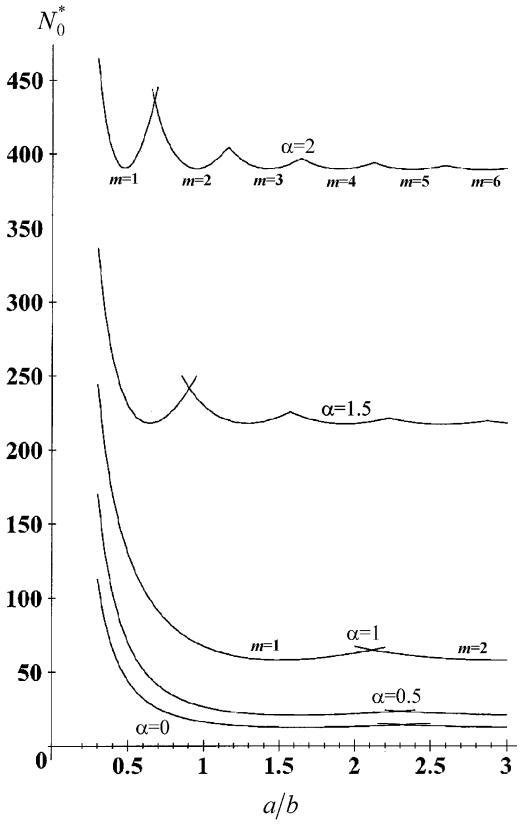

Fig. 5. Nondimensional buckling in-plane loads $N_0^* \equiv N_0 b^2/D$ vs. aspect ratio $k \equiv a/b$ for S-C-S-F plates ($\nu = 0.3$).

$$Y_m^{\mathrm{IV}} - 2\beta_m^2 Y_m'' + [\beta_m^4 - N_0^*(1-\alpha\eta)\beta_m^2]Y_m = 0, \tag{7}$$

where Y_m^{IV} and Y_m'' are the fourth and second derivatives of Y_m with respect to η, respectively, β_m is defined by

$$\beta_m \equiv \frac{m\pi}{k} \quad (m = 1, 2, 3, \ldots), \tag{8}$$

and N_0^* is the nondimensional compressive force at the edge $y = 0$, defined by

$$N_0^* \equiv \frac{N_0 b^2}{D}. \tag{9}$$

Eq. (7) is an ordinary differential one in η for each m. The ordinary differential equation has one variable coefficient in it, but it may be solved exactly by the power series solution method of Frobenius (Wylie, 1951).

Let us assume the deflection function as

$$Y_m(\eta) = \sum_{n=0}^{\infty} C_{m,n}\eta^n, \tag{10}$$

where $C_{m,n}$ is an arbitrary coefficient. Substituting Eq. (10) into Eq. (7), we obtain

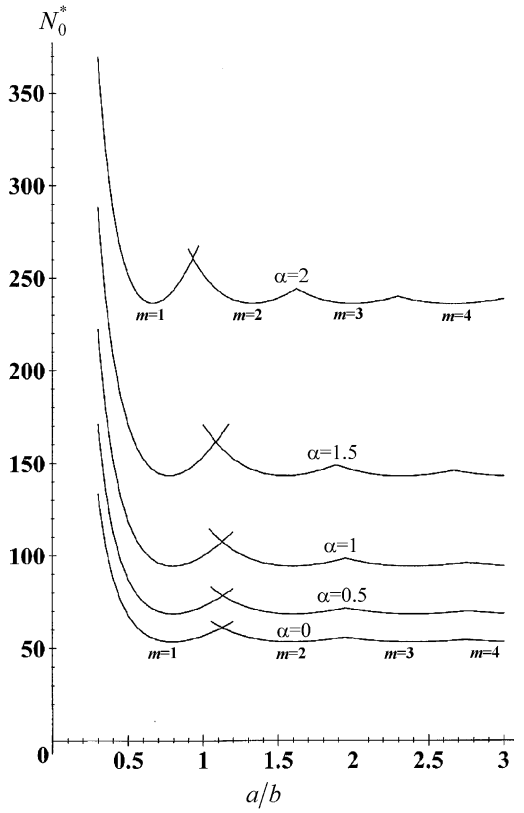

Fig. 6. Nondimensional buckling in-plane loads $N_0^* \equiv N_0 b^2/D$ vs. aspect ratio $k \equiv a/b$ for S-S-S-C plates (all ν).

$$\sum_{n=4}^{\infty} n(n-1)(n-2)(n-3)C_{m,n}\eta^{n-4} - 2\beta_m^2 \sum_{n=2}^{\infty} n(n-1)C_{m,n}\eta^{n-2} + \beta_m^2(\beta_m^2 - N^*)\sum_{n=0}^{\infty} C_{m,n}\eta^n + \alpha\beta_m^2 N_0^* \sum_{n=0}^{\infty} C_{m,n}\eta^{n+1} = 0 \tag{11}$$

Shifting indices, Eq. (11) becomes

$$\sum_{n=0}^{\infty}[\{(n+4)(n+3)(n+2)(n+1)C_{m,n+4} - 2\beta_m^2(n+2)(n+1)C_{m,n+2} + \beta_m^2(\beta_m^2 - N^*)C_{m,n}\}\eta^n + \alpha\beta_m^2 N_0^* C_{m,n}\eta^{n+1}] = 0 \tag{12}$$

Using the property of identity, for the coefficient of η^0,

$$C_{m,4} = \frac{\beta_m^2}{24}\left[4C_{m,2} - (\beta_m^2 - N_0^*)C_{m,0}\right], \tag{13}$$

and for the coefficients of $\eta^n (n = 1, 2, 3, \ldots)$

$$C_{m,n+4} = \frac{[2(n+2)(n+1)C_{m,n+2} - (\beta_m^2 - N_0^*)C_{m,n} - \alpha N_0^* C_{m,n-1}]\beta_m^2}{(n+4)(n+3)(n+2)(n+1)}. \tag{14}$$

Eqs. (13) and (14) are the recursion relationships for $C_{m,n}$ when $n \geqslant 4$.

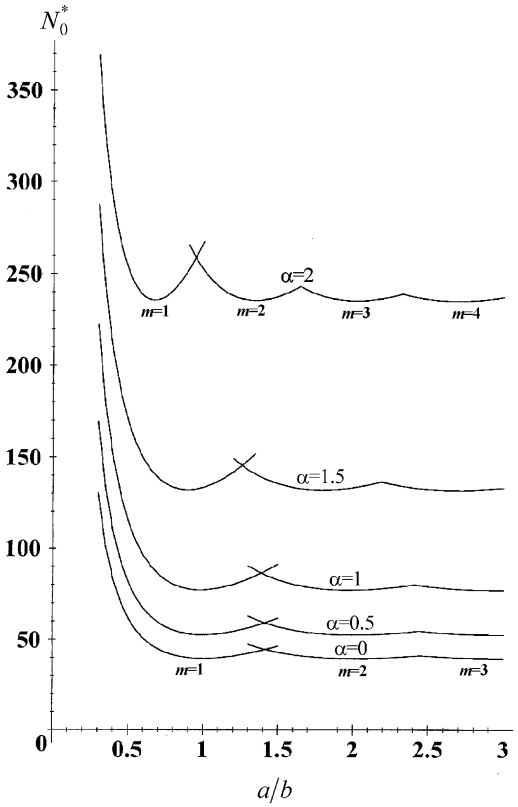

Fig. 7. Nondimensional buckling in-plane loads $N_0^* \equiv N_0 b^2/D$ vs. aspect ratio $k \equiv a/b$ for S-S-S-S plates (all ν).

Thus $C_{m,0}$, $C_{m,1}$, $C_{m,2}$, and $C_{m,3}$ are arbitrary coefficients, which will be used in two boundary conditions at each side ($\eta = 0$ and 1), and the other coefficients $C_{m,n}$, for $n \geqslant 4$ are expressed in terms of them. Typically, the four boundary conditions yield four homogeneous equations with unknowns $C_{m,0}$, $C_{m,1}$, $C_{m,2}$, and $C_{m,3}$. To obtain a non-trivial solution of the system, the determinant of the matrix of the coefficients is set to zero for the nondimensional buckling loads (N_0^*). One sees that the elements of the matrix have infinite series in them. Substituting each N_0^* back into the four homogeneous equations yields the corresponding eigenvectors, $C_{m,n}/C_{m,0}$ (with $n = 1, 2, 3$), which determines the mode shape.

There are three physically meaningful, simple types of boundary conditions along the edges $\eta = 0$ and $\eta = 1$ for which this solution may be used:

$$\text{Clamped} : w = 0 \text{ and } \frac{\partial w}{\partial y} = 0 \Rightarrow Y_m = Y'_m = 0 \tag{15a}$$

$$\text{Simply supported} : w = 0 \text{ and } M_y = 0 \Rightarrow Y_m = Y''_m = 0 \tag{15b}$$

$$\text{Free} : M_y = 0 \text{ and } V_y = 0 \Rightarrow Y''_m = Y'''_m + m^2\pi^2(2-\nu)Y'_m = 0 \tag{15c}$$

where $M_y = 0$ and $V_y = 0$ are bending moment and effective shear force per unit distance on the y-plane, respectively. Substituting Eq. (10) into one of the sets of boundary condition (15) for each of the two edges,

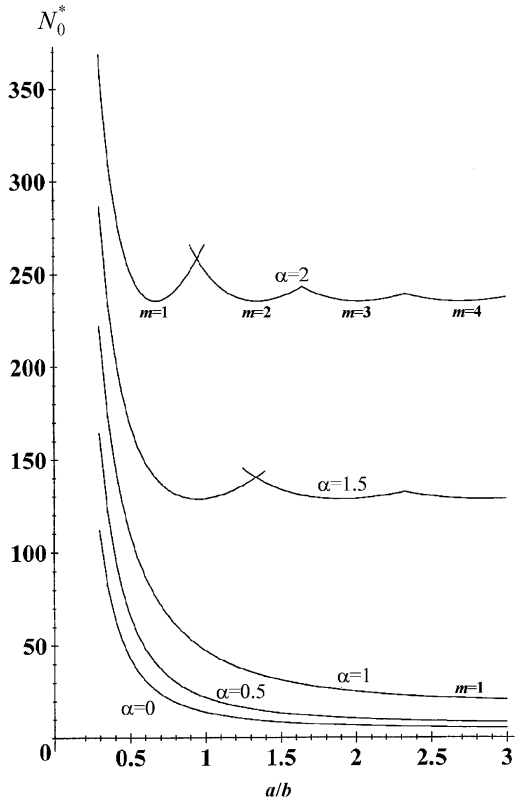

Fig. 8. Nondimensional buckling in-plane loads $N_0^* \equiv N_0 b^2/D$ vs. aspect ratio $k \equiv a/b$ for S-S-S-F plates ($v = 0.3$).

$\eta = 0$ and $\eta = 1$, yields the fourth order characteristic determinant described earlier from which an infinite set of eigenvalues (nondimensional buckling loads, N_0^*) may be found for each longitudinal half-wave number (m). The lowest value among all these N_0^* corresponds to the nondimensional critical buckling load $N_{0\mathrm{cr}}^*$. In certain special cases, the determinant quickly reduces to a lower order one.

3. Convergence

The exact solution functions given by Eq. (10) require summing an infinite series. Depending upon the degree of accuracy which one wants to have in numerical calculations, the upper limit of the summation is truncated at a finite number (N), which may be as large as needed. This procedure is no different than that followed in the evaluation of other transcendental functions arising in the exact solutions of other boundary value problems (e.g., trigonometric, hyperbolic, Bessel, Hankel).

To examine the convergence rate of the power series of Eq. (10), as well as to establish the correctness of the results, the present equations are applied to the buckling problems of plates with aspect ratio (a/b) of 2.3, for all nine possible, but distinct, combinations of the boundary conditions described by Eqs. (15), and the convergence studies are exhibited in Table 1 for the nondimensional critical buckling moments $M_{\mathrm{cr}}^* (= N_{0\mathrm{cr}}^*/6)$ for $\alpha = 2$ and $v = 0.3$. The free, simply supported, and clamped edge conditions are abbreviated to F, S, and C, respectively in Table 1.

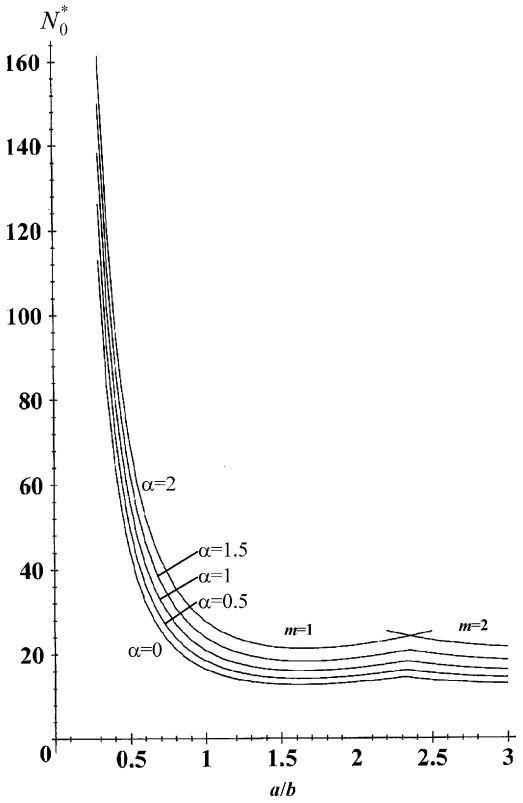

Fig. 9. Nondimensional buckling in-plane loads $N_0^* \equiv N_0 b^2/D$ vs. aspect ratio $k \equiv a/b$ for S-F-S-C plates ($\nu = 0.3$).

Table 1 shows that the S-F-S-C plate (see Fig. 1) has a much lower critical moment ($M_{cr}^* = 3.925$) than that of the S-C-S-F plate ($M_{cr}^* = 65.11$). This is because in the former case the compression part of the plate is in the vicinity of the free edge ($y = 0$), whereas in the latter the buckling is resisted by the fixed edge ($y = 0$). One also observes in Table 1 that the critical buckling mode shape of the S-F-S-C plate has only one half-wave ($m = 1$) in the loaded (x) direction, whereas the S-C-S-F plate has five. It is seen that more terms of the power series are needed to represent the plate deformations properly for four-digit convergence when more half-waves are in the mode shape.

It is interesting to note that the convergence is not monotonic. That is, the eigenvalues (N_0^*) oscillate about the exact values as N is increased, rather than approaching them from one direction. The underlined numbers in the table are those beyond which the fourth digit does not change as N increases. As more terms are taken the buckling loads converge to their exact values. Data is not given in Table 1 for certain small numbers of terms because of the difficulty of the computer in establishing the roots of the characteristic determinant in these cases.

The numerical results from the power series approach which will be presented in Section 4 were obtained by taking sufficient terms (N) to converge to the number of digits shown in the tables. Typically, this was $N = 50$.

Additional convergence studies for the S-F-S-F plates (Kang and Leissa, 2001) with $\alpha = 2$ (pure end moments) and S-C-S-C plates (Leissa and Kang, 2002) with $\alpha = 0$, 1, 2, and having various aspect ratios (a/b) are also available.

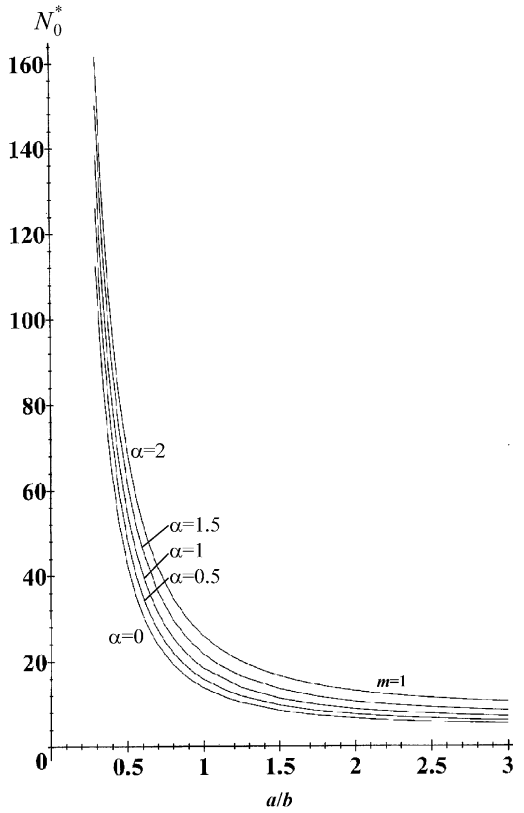

Fig. 10. Nondimensional buckling in-plane loads $N_0^* \equiv N_0 b^2/D$ vs. aspect ratio $k \equiv a/b$ for S-F-S-S plates ($v = 0.3$).

4. Buckling loads and mode shapes

It is interesting to observe how the critical buckling load varies as α changes for each boundary condition. Examples of this are shown in Figs. 3–11, where $N_0^* \equiv N_0 b^2/D$ are plotted versus for the linearly varying edge loadings exhibited in Fig. 2 ($\alpha = 0$, 0.5, 1, 1.5, 2), for plates having all nine possible combinations of clamped (C), simply supported (S) or free (F) edges at $y = 0$ and b; S-C-S-C, S-C-S-S, S-C-S-F, S-S-S-C, S-S-S-S, S-S-S-F, S-F-S-C, S-F-S-S, and S-F-S-F plates, respectively. These figures show the fact that the critical mode shape has an increasing number (m) of longitudinal half waves as the length-to-width ratio (a/b) increases. The critical modes all have only one partial wave in the y-direction.

As one increases α the buckling load parameter $N_0 b^2/D$ is seen to increase, as expected, because for a fixed N_0 the longitudinal force (i.e., the integral of σ_x over the plate width) decreases. Not only do the curves shift upward with increasing α, but the number of longitudinal half-waves increases with two exceptions of S-F-S-S (in Fig. 10) and S-F-S-F (Fig. 11); for example, with $a/b = 2.8$ the critical mode shape changes from $m = 2$ for $\alpha = 0$, 0.5,1, to $m = 4$ for $\alpha = 1.5$, to $m = 6$ for $\alpha = 2$ for S-C-S-F (in Fig. 5). It is interesting to note from Fig. 10 that considering the results of $N_0^* \equiv N_0 b^2/D$ for, $a/b > 3$ the critical buckling modes for S-F-S-S plates always have $m = 1$ irrespective of α and a/b, like the S-F-S-F plates in Fig. 11 (Kang and Leissa, 2001).

It is observed in Figs. 3–5 that the buckling curves of $N_0^* \equiv N_0 b^2/D$ are almost identical for $\alpha = 2$ (in-plane moments) if the compression side of the plate is clamped (S-C-S-C, S-C-S-S, S-C-S-F), no matter

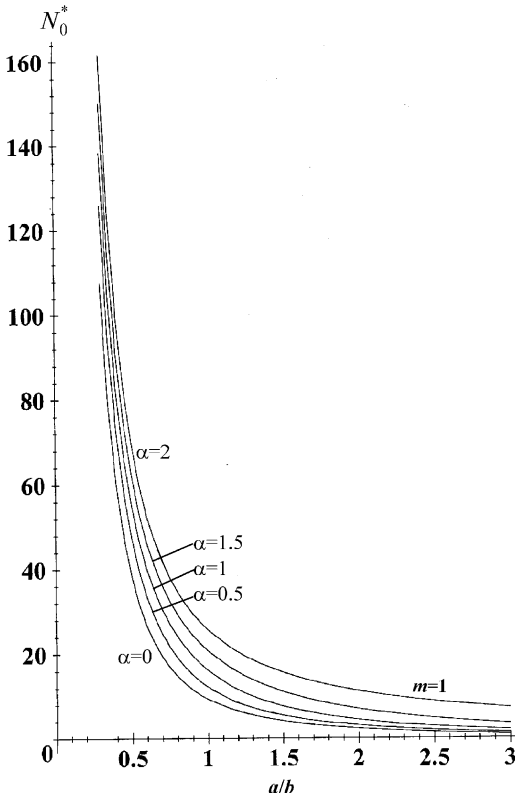

Fig. 11. Nondimensional buckling in-plane loads $N_0^* \equiv N_0 b^2/D$ vs. aspect ratio $k \equiv a/b$ for S-F-S-F plates ($\nu = 0.3$).

whether the other edge ($y = b$) is restrained or not. This was also seen in Table 1 where the convergent values of $M_{cr}^* = 65.12$ or 65.11 are almost identical (for the particular aspect ratio, a/b, of 2.3). This can be partially explained physically as the tensile stress in one half ($b/2 < y \leqslant b$) stabilizes the plate while the compressive stress in $0 \leqslant y < b/2$ destabilizes it, with both effects virtually negating each other if the compression edge is clamped. Accordingly, one sees slight differences among the curves of Figs. 3–5 for $\alpha = 1.5$, when only a small part of the plate is in tension (Fig. 2). When the compression edge ($y = 0$) is only simply supported, losing the slope constraint, slight differences can be seen in the curves for $\alpha = 2$ in Figs. 6–8. And the convergent values in Table 1 for the three cases are more distinct (40.06, 39.83, 39.75). For the remaining three cases (S-F-S-C, S-F-S-S, S-F-S-F) the compressive edge is free, and considerable differences are seen among the curves for $\alpha = 2$ in Figs. 9–11.

Table 2
Minimum buckling loads $N_0^* \equiv N_0 b^2/D$ for edge conditions not directly affected by ν

Edge conditions	α				
	0	0.5	1	1.5	2
S-C-S-C	68.80	91.43	133.7	224.3	390.4
S-C-S-S	53.39	73.64	115.8	218.5	390.4
S-S-S-C	53.39	68.48	94.18	143.2	236.3
S-S-S-S	39.48	52.49	77.08	132	235.7

Table 3
Minimum buckling loads $N_0^* \equiv N_0 b^2/D$ for edge conditions directly affected by v

Edge conditions	v	α				
		0	0.5	1	1.5	2
S-C-S-F	0	15.09	24.69	64.24	217.6	390.3
	0.3	12.64	20.91	58.59	218.0	390.3
	0.5	10.40	17.35	50.49	218.2	390.3
S-S-S-F	0	6.000	9.600	24.00	127.3	235.5
	0.3	4.200	6.700	16.80	128.6	235.4
	0.5	3.000	4.800	12.00	129.3	235.3
S-F-S-C	0	15.09	16.94	19.26	22.24	26.15
	0.3	12.64	14.08	15.88	18.16	21.10
	0.5	10.40	11.53	12.93	14.68	16.93
S-F-S-S	0	6.000	6.857	8.000	9.600	12.00
	0.3	4.200	4.800	5.600	6.720	8.400
	0.5	3.000	3.429	4.000	4.800	6.000

Table 4
Critical buckling loads $N_{0\mathrm{cr}}^* \equiv N_0 b^{2\mathrm{cr}}/D$ for S-F-S-F plates

a/b	v	α				
		0	0.5	1	1.5	2
0.5	0	39.48	49.68	59.17	68.28	77.76
	0.3	38.42	47.62	55.26	62.43	69.78
	0.5	35.66	43.23	48.77	53.97	59.33
1	0	9.870	12.95	17.56	23.54	30.31
	0.3	9.399	12.27	16.21	20.79	25.73
	0.5	8.352	10.84	13.98	17.35	20.89
2	0	2.467	3.277	4.774	7.911	13.82
	0.3	2.292	3.040	4.389	6.990	11.26
	0.5	1.949	2.583	3.702	5.738	8.816
5	0	0.3948	0.5261	0.7853	1.508	5.365
	0.3	0.3608	0.4807	0.7165	1.360	4.296
	0.5	0.2992	0.3986	0.5935	1.118	3.309
10	0	0.09870	0.1316	0.1971	0.3900	2.670
	0.3	0.08991	0.1199	0.1795	0.3541	2.133
	0.5	0.07422	0.09894	0.1481	0.2916	1.638

Tables 2 and 3 present the minimum buckling loads $N_0^* \equiv N_0 b^2/D$ over the entire spectrum of a/b for edge conditions not directly affected by v such as S-C-S-C, S-C-S-S, S-S-S-C, S-S-S-S plates, and for ones directly affected by v such as S-C-S-F, S-S-S-F, S-F-S-C, S-F-S-S plates for $v = 0, 0.3, 0.5$, respectively. These minimum values are the most important values of the spectrum because if the loading does not exceed the minimum buckling load, then the plate cannot buckle, regardless of a/b. It is noted that the minimum results for S-F-S-F are omitted in Table 3 because the S-F-S-F plate has minimum of zero at $a/b = \infty$.

The case of the S-F-S-F plate is a particularly important one. Table 4 displays critical buckling loads for $N_{0\mathrm{cr}}^* \equiv N_{0\mathrm{cr}} b^2/D$ such plates having various $a/b = 0.5$, 1, 2, 5, 10, a variety of linearly varying loadings ($\alpha = 0$, 0.5, 1, 1.5, 2, as in Fig. 2), and the full range of possible Poisson's ratios for an isotropic material ($v = 0$, 0.3, 0.5). For $\alpha = 0$ (uniform loading) and $v = 0$, one observes that the critical buckling load is exactly that of an Euler column $\pi^2/(a/b)^2$; that is, for $v = 0$, there is no transverse (y) curvature in the mode

Table 5
Comparison of nondimensional buckling moments $M^* \equiv M/D$ of S-S-S-C plates with in-plane moments ($\alpha = 2$) for $m = 1$

Method	a/b									
	0.4	0.5	0.6	0.65	0.66	0.67	0.7	0.8	0.9	1.0
Nölke	48.5	42.8	40.55	40.27	40.27	40.27	40.38	41.57	43.69	46.62
Power series	47.87	42.00	39.72	39.40	39.38	39.38	39.47	40.56	42.64	45.51

shape. Nonzero ν induces transverse curvature (i.e., anticlastic bending). It would appear from Table 4 that increasing ν causes decreased N_{0cr}, but that is not the case, for $D \equiv Eh^3/12(1-\nu^2)$ depends upon ν. A proper comparison of load parameters ($12N_{0cr}b^2/Eh^3$) shows with $a/b = 1$ and $\alpha = 0$, for example, that the parameter $12N_{0cr}b^2/Eh^3$ increases from 9.870 to 11.14 by 12.8 percent as ν increases from 0 to 0.5.

Table 5 compares the nondimensional buckling moments $M^*(\equiv M/D = N_0^*/6)$ of S-S-S-C plates with pure in-plane moments ($\alpha = 2$) for $m = 1$ obtained by Nölke (1937) using an energy method. In all cases, Nölke's results are larger (but within 2.5%) than the exact ones from the present power series method. Table 6 compares nondimensional critical buckling loads N_{0cr}^* of S-S-S-S plates having various loading conditions ($\alpha = 2$, 4/3, 1, 4/5, 2/3) obtained by Timoshenko (1921, 1934) using an energy method with those found with the present, exact power series solution. In most cases the three or two digit results obtained by Timoshenko agree with the exact results up to three or two significant figures with some exceptions, in particular for $\alpha = 2/3$, where there are large disagreements. Table 7 also compares M_{cr}^* of S-S-S-S plates with pure in-plane moment ($\alpha = 2$) obtained approximately by Stein (1934) and Chwalla (1940) with the exact results. Ban (1935) obtained the critical buckling loads for S-F-S-S and S-S-S-F plates for $\alpha = 1$, but comparisons are not made due to his highly inaccurate results, which will not be repeated here. Additional comparisons for the S-F-S-F plates (Kang and Leissa, 2001) with $\alpha = 2$ (pure end moments) and S-C-S-C plates (Leissa and Kang, 2002) with $\alpha = 0, 1, 2$, and having various aspect ratios (a/b) have already made elsewhere.

The buckling loads displayed in Tables 6 and 7 are critical values. That is, they are the lowest ones of the doubly infinite set of buckling eigenvalues that arise for each α and a/b. For example, when $\alpha = 1$ in Table

Table 6
Comparison of nondimensional critical buckling loads $N_{0cr}^* \equiv N_{0cr}b^2/D$ of S-S-S-S rectangular plates with linearly varying in-plane loading applied to each of the simply supported ends acting in the plane of the plate

α	Method	a/b								
		0.4	0.5	0.6	0.667	0.75	0.8	0.9	1.0	1.5
2	Timoshenko	287	253	238	236	238	241	253	253	238
	Power series	287.2 ($m = 1$)	252.0 ($m = 1$)	238.1 ($m = 1$)	235.7 ($m = 1$)	238.0 ($m = 1$)	241.5 (m=1)	252.4 ($m = 1$)	252.0 ($m = 2$)	238.0 ($m = 2$)
4/3	Timoshenko	185	–	127	–	114	111	–	109	114
	Power series	186.3 ($m = 1$)	148.5 ($m = 1$)	128.1 ($m = 1$)	119.8 ($m = 1$)	113.3 ($m = 1$)	110.9 ($m = 1$)	108.5 ($m = 1$)	108.7 ($m = 1$)	113.3 ($m = 2$)
1	Timoshenko	149	–	96	–	83	80	–	77	83
	Power series	149.5 ($m = 1$)	114.7 ($m = 1$)	96.16 ($m = 1$)	88.60 ($m = 1$)	82.59 ($m = 1$)	80.26 ($m = 1$)	77.66 ($m = 1$)	77.10 ($m = 1$)	82.59 ($m = 2$)
4/5	Timoshenko	131	–	82	–	70	68	–	65	70
	Power series	113.4 ($m = 1$)	99.3 ($m = 1$)	82.44 ($m = 1$)	75.62 ($m = 1$)	70.20 ($m = 1$)	68.09 ($m = 1$)	65.70 ($m = 1$)	65.09 ($m = 1$)	70.20 ($m = 2$)
2/3	Timoshenko	107	–	70	–	60	59	–	57	60
	Power series	120.8 ($m = 1$)	90.69 ($m = 1$)	74.98 ($m = 1$)	68.66 ($m = 1$)	63.64 ($m = 1$)	61.68 ($m = 1$)	59.45 ($m = 1$)	58.86 ($m = 1$)	63.64 ($m = 2$)

Table 7
Comparison of nondimensional critical buckling moments $M^*_{cr} \equiv M_{cr}/D$ of S-S-S-S rectangular plates for $\alpha = 2$

Method	a/b									
	0.3 ($m = 1$)	0.4 ($m = 1$)	0.5 ($m = 1$)	0.6 ($m = 1$)	0.67 ($m = 1$)	0.8 ($m = 1$)	0.9 ($m = 1$)	1.0 ($m = 2$)	1.2 ($m = 2$)	1.5 ($m = 2$)
Stein	61.5	47.9	41.9	39.6	39.3	40.1	42.1	41.9	39.6	39.6
Chwalla	61.6	47.6	41.9	39.7	39.3	39.3	39.3	39.3	39.3	39.3
Power series	61.61	47.87	41.99	39.68	39.28	40.25	42.07	41.99	39.68	39.66

6, for $a/b \leqslant 1$ the critical mode shape has a single half-wave in the x-direction ($m = 1$), and for $1.4 < a/b < 2.4$ the mode has $m = 2$. The nondimensional critical buckling loads N^*_{0cr} of S-S-S-S plates for $\alpha = 1$ are also seen in the middle curve appearing in Fig. 7.

The critical loads listed in Table 6 are only for the range of plate aspect ratio $0.4 \leqslant a/b \leqslant 1.5$. However, it should be noted that these are the values also for aspect ratios $m(a/b)$, where $m = 1, 2, 3, \ldots$. Thus for example, $N^*_{0cr} = 77.66$ for $\alpha = 1$ is the critical load for $a/b = 0.9$, 1.8, 2.7, 3.6, etc. This is seen, not only from the mathematical solution for the eigenvalues, but also by considering the mode shape described by Eq. (6). The function $\sin(m\pi\xi)$ is periodic in ξ. Considering, for example, $m = 3$, the simply supported edge conditions at $\xi = 0$ and 1 are duplicated at the node lines which appear in the mode shape at $\xi = 1/3$ and 2/3. It should also be noted that, for example, $N^*_0 = 149.5$ for $\alpha = 1$ is not only the critical load for $a/b = 0.4$; it is also is a buckling load for $a/b = 0.8(m = 2)$, $a/b = 1.2(m = 3)$, etc. However, it is not the critical load for the latter a/b.

Contour plots (lines of constant displacement) of the critical buckling mode shapes are displayed in Figs. 12, 13 for plates having $a/b = 2.3$ and 1, respectively, for $\alpha = 2$ and $\nu = 0.3$. In the figures, the critical mode shapes having an odd number of longitudinal half-waves ($m = 1,3,5$) are symmetric about the mid-axis $x = a/2$, while those having an even number ($m = 2,4$) are anti-symmetric. When m is equal or more than two, any part of the mode shapes divided by the vertical lines of zero displacements bulges out while the adjacent part(s) bulge(s) in. Fig. 12 shows clearly that the critical mode shape can change from $m = 1$ to 3 to 4 to 5 as the boundary conditions become increasing restrained. Additional contour plots of critical

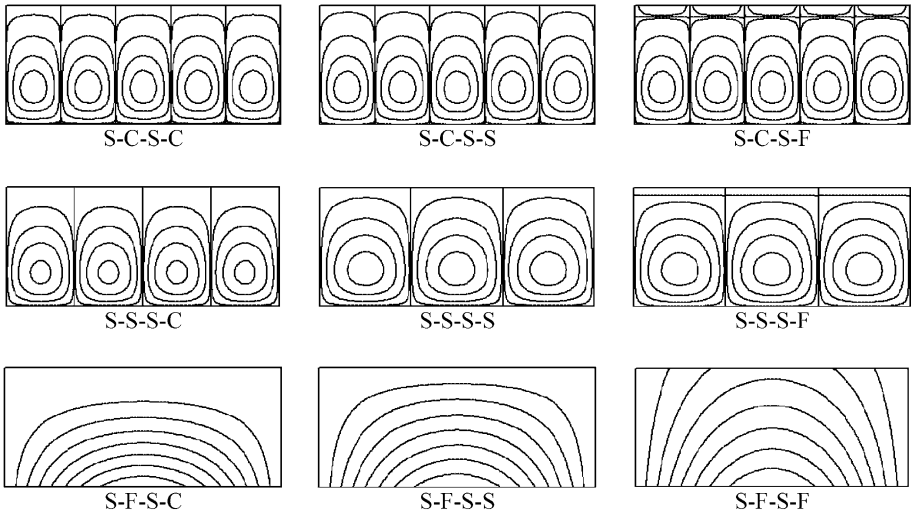

Fig. 12. Critical buckling mode shapes of rectangular plate loaded at two opposite ends simply-supported by in-plane moments ($\alpha = 2$) for $a/b = 2.3$ and $\nu = 0.3$.

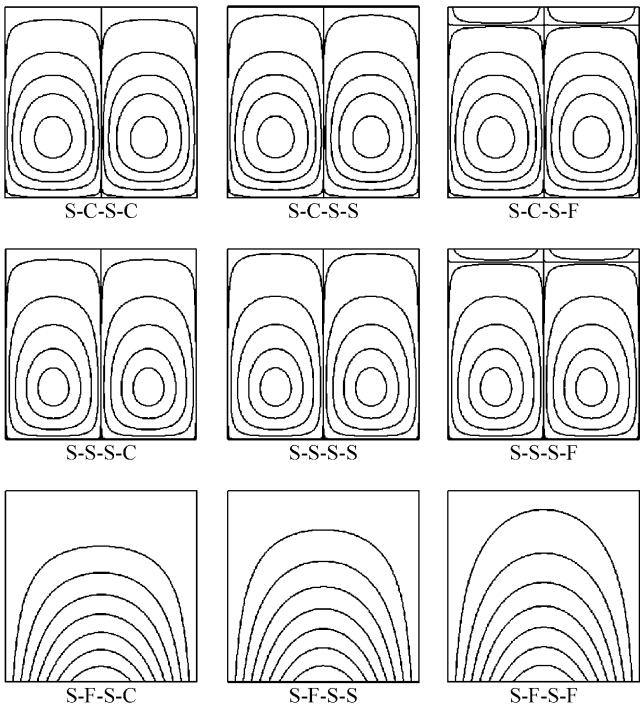

Fig. 13. Critical buckling mode shapes of rectangular plate loaded at two opposite ends simply-supported by in-plane moments ($\alpha = 2$) for $a/b = 1$ and $\nu = 0.3$.

buckling mode shapes for the S-F-S-F plates (Kang and Leissa, 2001) for $\alpha = 2$ (pure end moments) and S-C-S-C plates (Leissa and Kang, 2002) for $\alpha = 0, 1, 2$ having various aspect ratios (a/b) are also available elsewhere.

5. Conclusions

The foregoing work has shown how an exact solution procedure may be followed to obtain a variety of interesting and useful results for buckling loads and some of their corresponding mode shapes of rectangular plates having two opposite edges simply supported, with those edges being subjected to linearly varying in-plane stresses. The procedure was applied to all possible combinations of clamped, simply supported or free edge conditions applied continuously along the other unloaded edges at $y = 0$ and b. Additional, extensive results for the S-F-S-F plates (Kang and Leissa, 2001) having end moments only ($\alpha = 2$) and S-C-S-C plates (Leissa and Kang, 2002) for $\alpha = 0, 1, 2$ are also available elsewhere.

Assuming a sinusoidal displacement (w) in the x-direction resulted in a separation of variables (x and y), yielding an ordinary differential equation in y which had variable coefficients. An exact solution of this was obtained in terms of an infinite power series (i.e., the method of Frobenius). The infinite series are transcendental functions, similar to others commonly encountered in structural mechanics (e.g., trigonometric, hyperbolic, Bessel, Hankel) which are also evaluated as power series, except that present ones no "name" assigned to them.

As demonstrated by the results shown in Table 1, extreme care must be taken to use enough terms in the series to obtain accurate numerical results. Otherwise, very poor results may be obtained, even though as

many as 31 terms are used for some plates (e.g., S-C-S-C, S-C-S-S, S-C-S-F). This, of course, is a consideration when evaluating any functions expressed as power series. Also notable is the relatively wild character of the convergence. It is not monotonic, but oscillatory. Moreover, the oscillation amplitude does not necessarily decrease as terms as added. Most astonishingly, solutions could not even be established numerically for small numbers of terms because of the extreme oscillation then present. However, as Table 1 shows, as sufficient terms of the polynomials are used, the buckling loads converge correctly, and exactly.

Besides the clamped, simply supported or free edge conditions along the edges $y = 0$ and b, these edges could also be restrained elastically (but uniformly) by adjacent support structure, in both transverse displacement and/or rotation, and the solution procedure would proceed straightforwardly.

If the in-plane edge loading were more general than linearly varying (i.e.,$N_x = f(y)$), then the exact procedure shown here could not be used. One would first have to solve a plane elasticity problem to determine N_x, N_y, and N_{xy} within the plate as functions of x and y. However, the variables separable solution assumed for w in Eq. (6) would not satisfy Eq. (1) for these N_x, N_y, and N_{xy}.

On the other hand, a more general solution than that shown here could be obtained by the present method if uniform in-plane loading were applied to the edges $y = 0$ and b (i.e., $N_y = \text{constant}$), in addition to the linearly varying of Eq. (3). After utilizing (6), the governing ordinary differential equation (7) would have one extra term in Y^n, but it could be solved exactly by assuming (10), and then following the procedure in the present work subsequent to (10).

References

Ban, S., 1935. Knickung der rechteckigen Platten bei veränderlicher Randbelastung. Abhandl. 4 te Int. Kongr, Brückbau u. Hockbau, Bd. 3, S.1–S.18.

Bassily, S.F., Dickinson, S.M., 1972. Buckling and lateral vibration of rectangular plates subject to in-plane loads –a Ritz approach. Journal of Sound Vibration 22 (2), 219–239.

Bassily, S.F., Dickinson, S.M., 1978. Buckling and vibration of in-plane loaded plates treated by a unified Ritz approach. Journal of Sound Vibration 59 (1), 1–14.

Bradford, M.A., Smith, S.T., Oehlers, D.J., 2000. Semi-compact steel plates with unilateral restraint subjected to bending, compression and shear. Journal of Constructional Steel Research 56, 47–67.

Brush, D.O., Almroth, B.O., 1975. Buckling of Bars, Plates and Shells. McGraw-Hill, New York.

Bulson, P.S., 1970. The Stability of Flat Plates. Chatto & Windus, London.

Chwalla, E., 1940. Erläuterungen zür Begründung des Normblattentwurfes. Knick-und Beulvorschriften für Stahlbau DIN E 4114.

Dickinson, S.M., 1978. The buckling and frequency of flexural vibration of rectangular isotropic and orthotropic plates using Rayleigh's method. Journal of Sound Vibration 61 (1), 1–8.

Japan Column Research Council, 1971. Handbook of Structural Stability. Corona Publishing Company, Tokyo.

Kaldas, M.M., Dickinson, S.M., 1981. Vibration and buckling calculations for rectangular plates subject to complicated in-plane stress distributions by using numerical integration in a Rayleigh-Ritz analysis. Journal of Sound Vibration 75 (2), 151–162.

Kang, J.-H., Leissa, A.W., 2001. Vibration and buckling of SS-F-SS-F rectangular plates loaded by in-plane moments. International Journal of Stability and Dynamics 1 (4), 527–543.

Kielb, R.E., Han, L.S., 1980. Vibration and buckling of rectangular plates under in-plane hydrostatic loading. Journal of Sound and Vibration 70 (4), 543–555.

Leissa, A.W., Kang, J.-H., 2002. Exact solutions for vibration and buckling of an SS-C-SS-C rectangular plate loaded by linearly varying in-plane stresses. International Journal of Mechanical Sciences 44, 1925–1945.

Nölke, K., 1937. Biegungsbeulung der Rechteckplatte. Ingineur Archiv 8, 403.

Smith, S.T., Bradford, M.A., Oehlers, D.J., 1999a. Local buckling of side-plated reinforced-concrete beams, I: Theoretical study. ASCE Journal of Structural Engineering 125 (6), 622–634.

Smith, S.T., Bradford, M.A., Oehlers, D.J., 1999b. Local buckling of side-plated reinforced-concrete beams, II: Experimental study. ASCE Journal of Structural Engineering 125 (6), 635–643.

Smith, S.T., Bradford, M.A., Oehlers, D.J., 2000. Unilateral buckling of elastically restrained rectangular mild steel plates. Computational Mechanics 26 (4), 317–324.

Stein, O., 1934. Die Stabilität der Blechträgerstehbleche im zweiachsigen Spannungszustand. Stahlbau 7, 57–60.

Szilard, R., 1974. Theory and Analysis of Plates: Classical and Numerical Methods. Prentice-Hall, Englewood Cliffs, New Jersey.

Timoshenko, S.P., 1921. Über die Stabilität versteifter Platten. Eisenbau 12, 147–163.
Timoshenko, S.P., 1934. The stability of the webs of plate girders. Eng'g 138, 207–209.
Timoshenko, S.P., Gere, J.M., 1963. Theory of Elastic Stability, 2nd ed. McGraw-Hill, New York.
Trahair, N.S., Bradford, M.A., 1998. The Behavior and Design of Steel Structures to AS4100, 3rd ed. E & FN Spon, London.
Volmir, A.S., 1967. Stability of Deformable Systems (in Russian). State Publishing House (Nauk), Moscow.
Wylie Jr., C.R., 1951. Advanced Engineering Mathematics. McGraw-Hill, New York.